ACS APPLIED MATERIALS & INTERFACES

Research Article

www.acsami.org

Actuating Porous Polyimide Films

Yaoming Zhang and Leonid Ionov*

Leibniz Institute of Polymer Research Dresden, Hohe Straße 6, D-01069 Dresden, Germany

Supporting Information

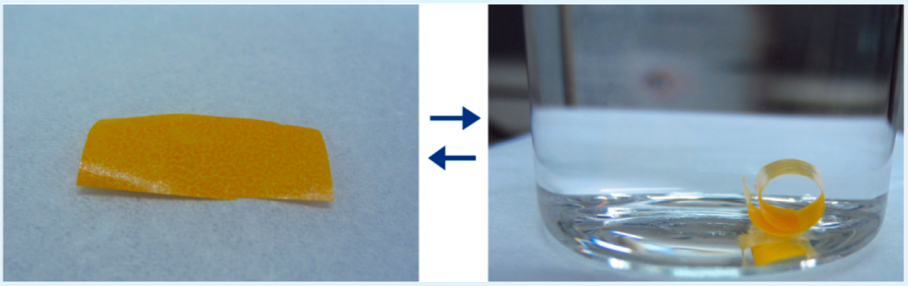

ABSTRACT: We report a novel method for the fabrication of one-component self-folding polymer films. The approach is based on films with a vertical gradient of porosity and was demonstrated on an example of porous polyimide films. The inhomogeneous porosity of the films was achieved through the implementation of capillary forces and gravity during the drying of a dispersion of colloidal particles in a solution of polymer precursor. As a result, three-layered films were formed. A monolayer of particles comprises the top layer, the second layer is the pure polymer, and the third layer is formed by a mixture of particles and polymer. Etching out the particles leaves polyimide film with inhomogeneous distributed pores. These porous polymer films roll and form tubes in organic solvents as well as their vapors and reversibly unfold in air. The obtained films were used for design of actuators, which are able to capture and release different objects through the reversible folding.

KEYWORDS: *self-folding, polyimide film, porous films, actuators*

INTRODUCTION

Self-folding films are a special sort of actuating systems, which are able to fold and form 3D structures in response to external stimuli.[1−4] Self-folding films typically consist of two kinds of materials with different volume expansion properties and their deformation mechanism resembles the bending of metal bilayers.[5] Recently, self-folding films were successfully applied for transport,[6] investigation of cell behavior in confinement,[7] nanooptics[8,9] energy storage elements,[10] scaffolds for tissue engineering,[11−14] and photovoltaic power applications.[15]

The ever-increasing trend in the field of self-folding films is on the area of self-folding films based on polymers.[16] In fact, the use of polymers provides many advantages such as various responsive properties, biocompatibility, biodegradability, and simplicity of fabrication.[17−22] Until now, most of the research in polymer self-folding films was focused on the development of self-folding films consisting of two components (polymers) that allowed, for example, development of self-folding films sensitive to different stimuli.[19,23−26] On the other hand, one material with different structure or cross-linking density is also expected to fold.[2,27,28] For example, Jamal et al. found that photo-cross-linked polymer SU-8 films with cross-linking gradient are able to reversibly bend due to the resolvation and desolvation.

In this paper, we report development of self-folding films based only on one polymer. For our approach, we have chosen polyimide (PI). PI has been widely applied in engineering fields due to its high thermal stability, high strain, and high chemical resistivity. PI, as a commercial product, has been widely used in aerospace, fibers, coatings, and electronic products, and could even be used as gas separation membranes.[29] Moreover, PI can be designed with various properties through chemically modify from monomer that allows design of a broad library of PI films.[30−35] To the best of our knowledge, there is no report on the self-folding of the high strain polymers such as polyimide.

EXPERIMENTAL SECTION

Materials. Pyromellitic dianhydride (PMDA), 4,4-oxidianiline (ODA), tetraethyl orthosilicate (TEOS), *N*,*N*-dimethylformamide (DMF), ammonium hydroxide (28%−30%), and hydrofluoric acid (HF, 30%) were purchased from Sigma-Aldrich and were used without purification.

Preparation of the Silica Particles. The silica particles (SiO_2) with sizes of 140 and 370 nm were prepared by the Stöber method (the morphology of the particles and size distribution, respectively, are shown in the Supporting Information, Table S1).[36] In a typical experiment for the synthesis of 140 nm large SiO_2 particles, 5.4 mL of TEOS was mixed with 120 mL of ethanol. Next, a mixture of 10 mL of ammonium hydroxide, 6.8 mL of deionized water, and 100 mL of ethanol was added to the TEOS solution. The mixture was stirred for 20 h at 25 °C to yield a milky solution. The obtained SiO_2 particles were centrifuged and washed by ethanol for several times. The particles were obtained after dry in vacuum oven at 40 °C for 12 h.

Received: February 6, 2014
Accepted: June 6, 2014
Published: June 6, 2014

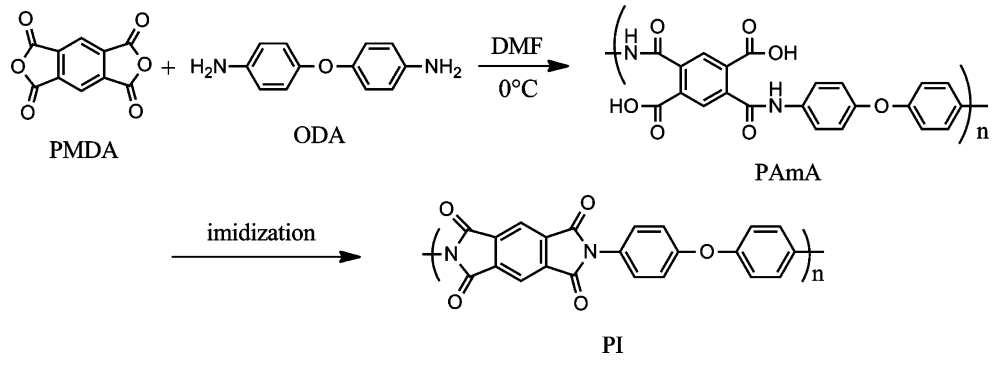

Figure 1. Synthesis process of the polyamide acid (PAmA) and polyimide (PI).

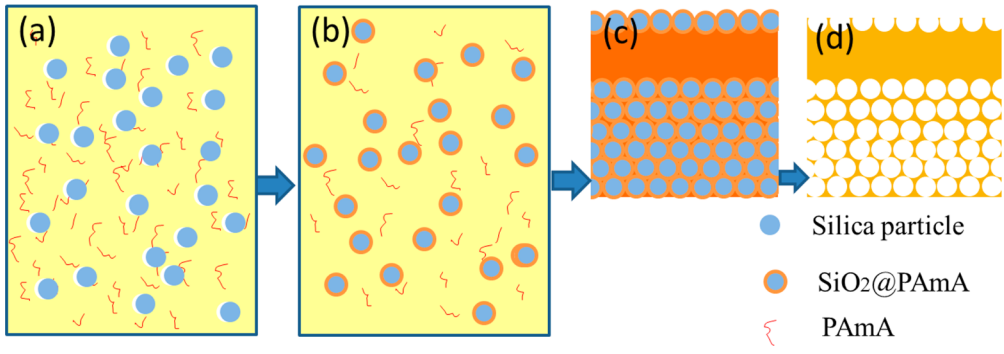

Figure 2. Scheme of fabrication of inhomogeneous polyimide porous film. (a) SiO_2 and PmAA solution in DMF, (b) SiO_2@PAmA and remained PAmA in DMF, (c) PAmA/SiO_2 film, and (d) inhomogeneous PI porous film.

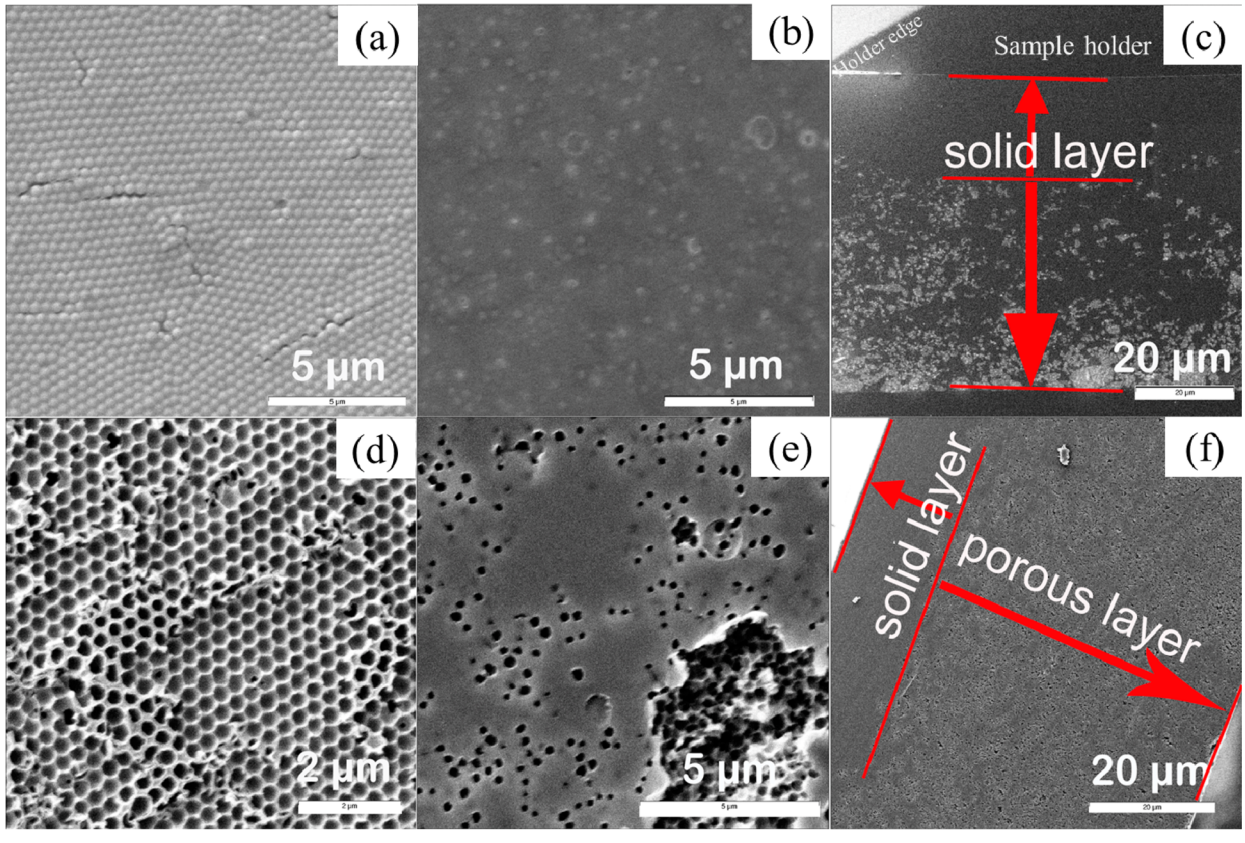

Figure 3. Morphology of PI/SiO_2 (upper panel) and PI porous (lower panel) films, respectively, prepared using 370 nm large SiO_2 particles, concentration 30%: (a and d) top view (b and e) bottom view, and (c and f) cross-section.

dx.doi.org/10.1021/am502492u | ACS Appl. Mater. Interfaces 2014, 6, 10072−10077

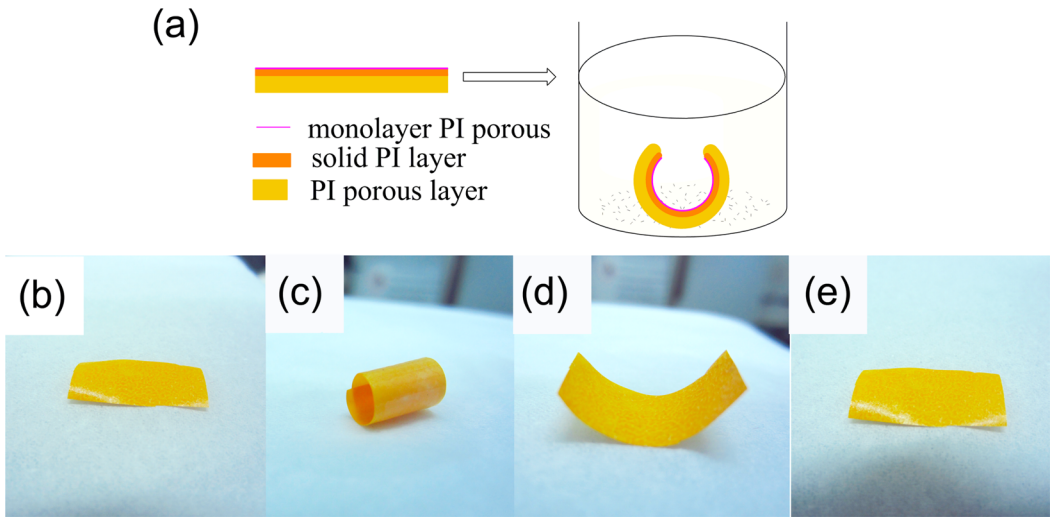

Figure 4. Scheme of the self-folding behavior in solvent (a), initial shape of the inhomogeneous PI porous film (b), rolled tube after the immersion in acetone for 1 min (c), shape recovery during exposure to air (d), and full recovery of the initial shape after 2 min of drying (e).

The size of the particle was controlled by adjusting the ratio between water, TEOS, and ammonium hydroxide.

Synthesis of Polyamide Acid (PAmA). The polyamide acid (PAmA) was prepared as described in ref 32 (Figure 1). Briefly, 3.350 g (16.73 mmol) of ODA dissolved in 60 mL of DMF. Then 3.722 g (17.06 mmol) of PMDA was added to the cold solution. The mixture was stirred by a mechanical stirrer under argon flow at 0−5 °C. The obtained solution was used as stock for further experiments. The typical molecular weight of the obtained polymer is ca. 40 000 g/mol[37]

Preparation of the Inhomogeneous Polyimide Films. An appropriate amount (10 wt % to 60 wt % for pure PAmA) of SiO_2 particles was mixed with 3 wt % of the PAmA solution in DMF. The mixture was sonicated in an ultrasonic bath for 2 h and stirred by a magnetic stirrer for another 24 h. The obtained solution was cast in a Petri dish and dried under vacuum at 80 °C for 12 h. The following annealing steps were used for imidazation: 80 °C for 1 h, 120 °C for 1 h, 180 °C for 1 h, and 240 °C for 1 h. Finally, the silica particles were etched out by 5% HF solution for 12 h to obtain the porous film. The thicknesses of the porous PI films were around 40 μm (measured by scanning electron microscopy (SEM)). The fraction of silica particles was varied to control the porosity of the films (for instance, PI-370 nm-30% means the inhomogeneous PI porous film was prepared using 30 wt % 370 nm large silica particles).

Swelling Degree Measurement. Swelling of solid PI and porous PI films was investigated by measuring the weight of the dry samples (m_d) and the weight of the sample incubated in acetone during different times (m_s). Swelling degree (SD) was calculated as SD = (m_s − m_d)/m_d.

RESULTS AND DISCUSSION

The folding polymer films were fabricated according to the approach illustrated in Figure 2. Briefly, silica particles were dispersed in PAmA solution in DMF to get a stable dispersion (Figure 2a,b). The solution was dried and inhomogeneous PAmA/SiO_2 film was formed during the drying process (Figure 2c). The inhomogeneous PI porous film (Figure 2d) was obtained after imidiazation of the polymer and removal of the particles.

We started with dispersing of SiO_2 particles in the solution of polyamide acid. The SiO_2 particles are well dispersible, as we believe, due to stabilization of particles by adsorbed PAmA chains. In fact, PAmA chains can readily adsorb on the particles surface due to formation hydrogen bonds.[38−40] The dangling tails of adsorbed PAmA chains, thus, form a solvated shell around the particles (SiO_2@PAmA) and stabilize them.

Drying of the polymer−particles dispersion at an elevated temperature starts at the solvent−air interface and slowly propagates inside the solution as the solvent gradually evaporates. It was found that some particles tend to accumulate at the liquid−air interface that resulted in the formation of a monolayer of the particles (as shown in Figure 3a). Considering that the density of the particles (d is ca. 2 g/cm^3) is larger than the density of the polymer solution (d = 0.959 g/cm^3), we propose that the reason for the aggregation of particles at the solvent−air interface is solvent convection and capillary forces between the particles.[41,42] On the other hand, due to their high mass density, most of the particles tend to sediment and assemble at the bottom, leaving the pure polymer solution above. Thus, the inhomogeneous film consists of three layers (i) a top single-layer of ordered particles with polymer, (ii) a middle layer of almost pure polymer with minor inclusions of particles, and (iii) a bottom layer of a composite particle−polymer mixture. Finally, the obtained three-layer polymer−particle films were annealed at elevated temperatures in order to convert PAmA into PI. The three layers are clearly visible in Figure 3a,b. The cross-section morphology shows the obvious difference between the solid upper layer and the particles-containing lower layer (Figure 3c).

The inhomogeneous PI porous film was formed after removal/etching of the particles with HF. SiO_2 is dissolved in HF while the PI remains intact. As shown in Figure 3, the morphologies of the top (Figure 3d) and the bottom of the film (Figure 3e) are different. The top is covered by one layer of the PI ordered pores, which are left after removal of hexagonally ordered particles. The bottom layer (Figure 3e) is the PI with pores left by particle aggregates (lower right in Figure 3e). The middle solid and the bottom porous layers are clearly seen in the SEM image of the cross-section of the PI film (Figure 3f). The top monolayer is, however, too thin to be observed from the cross-sectional surface.

We found that the PI porous films start to roll and form tubes upon immersion in acetone, as shown in Figure 4b,c. Rolling proceeds in a way that the porous layer is outward, forming a tube during rolling, and the solid polymer layer is inward (Figure 4a). Furthermore, the polymer films exhibit a

similar self-folding behavior when immersed in other solvents such as ethanol, chloroform, DMF, and their respective vapors. Reversible unfolding occurs when the film is taken away from the acetone and dried (as shown in Figure 4d,e). The developed method can also be applied for fabrication of inhomogeneous porous polyurethane (PU) films, which exhibit a self-folding behavior in water after solvated in acetone (as shown in the Supporting Information, Figure S1).

Next we investigated the mechanism of folding of PI films. It was found that solid, unstructured PI films swell slowly in acetone and their swelling degree reaches 14% after 3 days (as shown in Figure5). Contrary to that, porous PI films swell

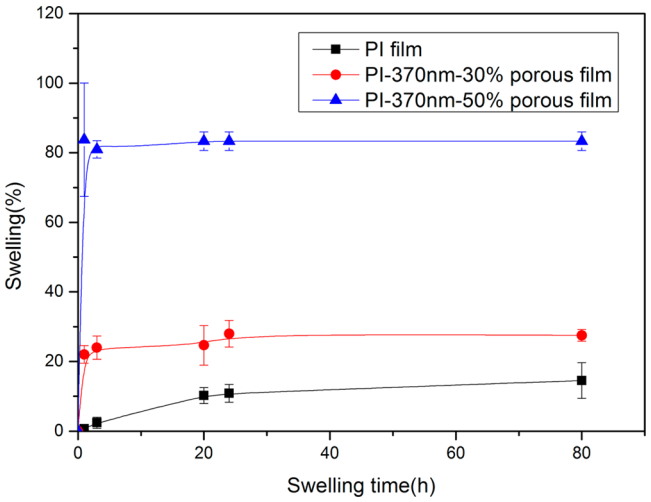

Figure 5. Swelling properties of the solid and porous PI films with different fraction of pores in acetone.

much faster and stronger. The swelling degree of the porous films reaches its saturation value after 10 s and remains nearly constant afterward. Apparently, porous PI films have a larger surface area than solid ones due to the abundant pores that cause fast diffusion of solvent molecules in the polymer and its faster swelling. Thus, porous and solid PI films swell with different rates and to different degrees. The pore size has also an effect on swelling degree. Films with more pores show higher swelling degrees. For example, the swelling degree of the PI-370 nm-50% film is ca. 85% whereas the swelling degree of the PI-370 nm-30% film is only 25%.

The observed swelling behavior explains the folding scenario. The porous part of the PI film swells faster and stronger than the solid part and, according to Timoshenko equation, the film bends in a way that the porous part is oriented outward and the solid part is oriented inward. Drying of the porous part of the film also occurs faster than for the solid part, which leads to unfolding of the film. This behavior of gradient porous PI films is similar to the behavior of SU-8 with a gradient of cross-linking densities.[28] Very interestingly, we noticed that the folded PI porous films unfold slightly after being exposed to acetone for a considerable amount of time (the slight unfolding process of the folded tube is shown in the Supporting Information, Figure S2). This effect can also be explained by the difference in the swelling rates of porous and solid parts. First, the porous part swells while the solid part does not, which results in folding. Subsequent swelling of the nonporous part of the film leads to unfolding of the film.

Next we investigated the effect of the fraction of pores and their sizes on the diameters of the formed tubes (Figure 6). We

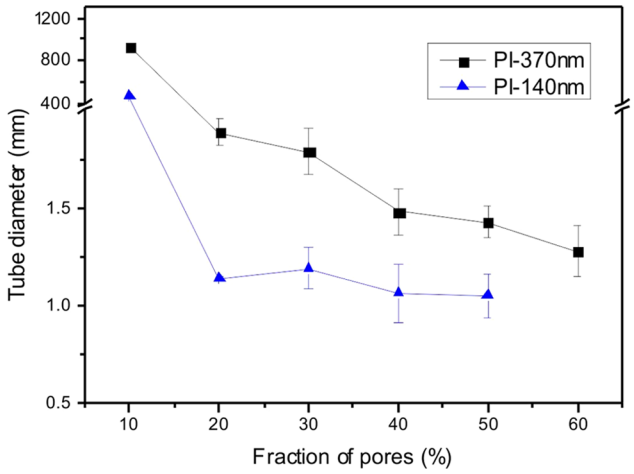

Figure 6. Correlation between diameter and the fraction of pores.

found that the films with the smallest fraction of pores (10%) slightly curl but do not form the tubes. Apparently, the thickness of the porous layer, which plays the role of active component here, is insufficient to completely roll the film. The films with a larger fraction of pores are able to completely roll and form the tubes. The diameter of the tubes gradually decreases with the increasing fraction of the pores. Size of the pores also plays a very important role. We found that the films with smaller pores tend to form tubes with smaller diameters (Figure 6). We propose that smaller pores provide larger surface area that enabled the films with high bending force from the swelling.

Finally, we demonstrated that porous PI films can be used for the design of actuators. The gripper actuator was assembled by gluing the inhomogeneous porous PI films between two solid PI films (as shown in Figure 7a). The flat film bended like a hinge when immersed in acetone and recovered to its initial shape after it was taken out of the solvent. The folding and unfolding are easily manipulated by approaching and removing the actuator from the organic solvent. This actuator could be repeatedly used for grabbing and releasing objects such as aluminum foil balls (20−30 mg). For example, an aluminum foil ball could be picked up in the acetone and then released in water (Figure 7c (Supporting Information, Movie S1). Because the polymer (PI) has high strain property, the gripper has potential application for a robot device (Figure S3 (Supporting Information) shows an actuator load object of about 10 g). The sensitivity of the solvent vapors was also used for the design of a propeller-shaped actuator by combining two pieces of PI porous film by their porous and solid sides (Figure 7b). The "propeller" is able to quickly fold when the film approaches the solvent and unfold when the solvent is removed and thus works like a mill (As shown in Figure 7d and Movie S2, Supporting Information). This may provide a new type of actuator to generate motion energy.

CONCLUSIONS

Inhomogeneous polyimide porous films, consisting of solid and porous parts, were prepared by using silica particles mixed with a polyimide precursor. Due to gravity and capillary forces, the mixture forms a three-layer structure where the topmost layer

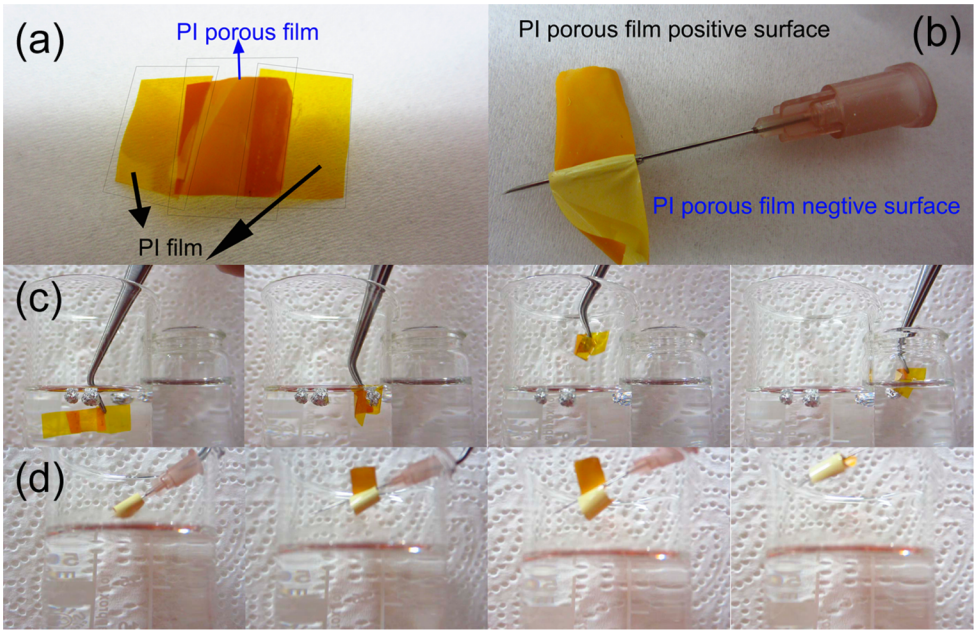

Figure 7. Photo of gripper actuator (a) and propeller-shaped actuator (b), the actuator grab an aluminum foil ball out from acetone and subsequently release it in water (c), and the propeller shaped actuator moving in acetone vapor (d).

consists of a particle monolayer, the second layer is a solid polymer, and the bottom layer is a composite particle−polymer mixture. A porous structure was formed after etching out of the particles. We demonstrated that the inhomogeneous porous film is able to fold and unfold reversibly in organic solvents/their vapors and air, respectively. The driving force of the folding is the different swelling degrees of the porous and nonporous parts of the film. The advantage of the demonstrated approach is the high thermal and mechanical stability of the used polymer−polyimide. The demonstrated approach, thus, opens new perspectives for the development of novel actuators.

■ ASSOCIATED CONTENT

Supporting Information

The size and distribution of silica particles that are used to prepare the porous films. Figure of showing the inhomogeneous PU cross-sectional morphology and the self-folded tubes. Picture of the folded tube slightly unrolling process during incubation in acetone. Picture of the actuator 1 loading the object about 10 g. Movie of the actuator for grab aluminum foil ball out acetone and release in water, and movie of propeller-shaped actuator self-folding behavior in vapor. This material is available free of charge via the Internet at http://pubs.acs.org.

■ AUTHOR INFORMATION

Corresponding Author

*L. Ionov. E-mail: ionov@ipfdd.de.

Author Contributions

The paper was written through contributions of all authors. All authors have given approval to the final version of the paper.

Notes

The authors declare no competing financial interest.

■ ACKNOWLEDGMENTS

We acknowledge the Alexander von Humboldt Foundation and DFG for financial support. The authors are thankful to Georgi Stoychev for critical comments on the paper.

■ REFERENCES

(1) Leong, T. G.; Zarafshar, A. M.; Gracias, D. H. Three-Dimensional Fabrication at Small Size Scales. *Small* **2010**, *6*, 792−806.
(2) Ionov, L. Biomimetic Hydrogel-Based Actuating Systems. *Adv. Funct. Mater.* **2013**, *23*, 4555−4570.
(3) Guan, J. J.; He, H. Y.; Lee, L. J.; Hansford, D. J. Fabrication of Particulate Reservoir-Containing, Capsulelike, and Self-Folding Polymer Microstructures for Drug Delivery. *Small* **2007**, *3*, 412−418.
(4) Pandey, S.; Ewing, M.; Kunas, A.; Nguyen, N.; Gracias, D. H.; Menon, G. Algorithmic Design of Self-Folding Polyhedra. *Proc. Natl. Acad. Sci. U. S. A.* **2011**, *108*, 19885−19890.
(5) Timoshenko, S. Analysis of Bi-Metal Thermostats. *J. Opt. Soc. Am.* **1925**, *11*, 233−255.
(6) Solovev, A. A.; Sanchez, S.; Pumera, M.; Mei, Y. F.; Schmidt, O. G. Magnetic Control of Tubular Catalytic Microbots for the Transport, Assembly, and Delivery of Micro-objects. *Adv. Funct. Mater.* **2010**, *20*, 2430−2435.
(7) Huang, G. S.; Mei, Y. F.; Thurmer, D. J.; Coric, E.; Schmidt, O. G. Rolled-Up Transparent Microtubes as Two-Dimensionally Confined Culture Scaffolds of Individual Yeast Cells. *Lab. Chip* **2009**, *9*, 263−268.
(8) Smith, E. J.; Liu, Z.; Mei, Y. F.; Schmidt, O. G. System Investigation of a Rolled-Up Metamaterial Optical Hyperlens Structure. *Appl. Phys. Lett.* **2009**, *95*, 083104.
(9) Schwaiger, S.; Broll, M.; Krohn, A.; Stemmann, A.; Heyn, C.; Stark, Y.; Stickler, D.; Heitmann, D.; Mendach, S. Rolled-Up Three-Dimensional Metamaterials with a Tunable Plasma Frequency in the Visible Regime. *Phys. Rev. Lett.* **2009**, *102*, 163903.
(10) Bof Bufon, C. C. s.; Cojal González, J. D.; Thurmer, D. J.; Grimm, D.; Bauer, M.; Schmidt, O. G. Self-Assembled Ultra-Compact Energy Storage Elements Based on Hybrid Nanomembranes. *Nano Lett.* **2010**, *10*, 2506−2510.
(11) Gracias, D. H.; Tien, J.; Breen, T. L.; Hsu, C.; Whitesides, G. M. Forming Electrical Networks in Three Dimensions by Self-Assembly. *Science* **2000**, *289*, 1170−1172.

(12) Leong, T.; Gu, Z. Y.; Koh, T.; Gracias, D. H. Spatially Controlled Chemistry Using Remotely Guided Nanoliter Scale Containers. *J. Am. Chem. Soc.* **2006**, *128*, 11336−11337.
(13) Randall, C. L.; Kalinin, Y. V.; Jamal, M.; Manohar, T.; Gracias, D. H. Three-Dimensional Microwell Arrays for Cell Culture. *Lab Chip* **2011**, *11*, 127−131.
(14) Jamal, M.; Bassik, N.; Cho, J. H.; Randall, C. L.; Gracias, D. H. Directed Growth of Fibroblasts into Three Dimensional Micropatterned Geometries via Self-Assembling Scaffolds. *Biomaterials* **2010**, *31*, 1683−1690.
(15) Guo, X. Y.; Li, H.; Ahn, B. Y.; Duoss, E. B.; Hsia, K. J.; Lewis, J. A.; Nuzzo, R. G. Two- and Three-Dimensional Folding of Thin Film Single-Crystalline Silicon for Photovoltaic Power Applications. *Proc. Natl. Acad. Sci. U. S. A.* **2009**, *106*, 20149−20154.
(16) Ionov, L. Soft Microorigami: Self-Folding Polymer Films. *Soft Matter* **2011**, *7*, 6786−6791.
(17) Kim, J.; Hanna, J. A.; Byun, M.; Santangelo, C. D.; Hayward, R. C. Designing Responsive Buckled Surfaces by Halftone Gel Lithography. *Science* **2012**, *335*, 1201−1205.
(18) Wu, Z. L.; Moshe, M.; Greener, J.; Therien-Aubin, H.; Nie, Z.; Sharon, E.; Kumacheva, E. Three-Dimensional Shape Transformations of Hydrogel Sheets Induced by Small-Scale Modulation of Internal Stresses. *Nat. Commun.* **2013**, *4*, 1586.
(19) Zakharchenko, S.; Sperling, E.; Ionov, L. Fully Biodegradable Self-Rolled Polymer Tubes: A Candidate for Tissue Engineering Scaffolds. *Biomacromolecules* **2011**, *12*, 2211−2215.
(20) Zakharchenko, S.; Puretskiy, N.; Stoychev, G.; Stamm, M.; Ionov, L. Temperature Controlled Encapsulation and Release Using Partially Biodegradable Thermo-Magneto-Sensitive Self-Rolling Tubes. *Soft Matter* **2010**, *6*, 2633−2636.
(21) Jamal, M.; Kadam, S. S.; Xiao, R.; Jivan, F.; Onn, T.-M.; Fernandes, R.; Nguyen, T. D.; Gracias, D. H. Bio-Origami Hydrogel Scaffolds Composed of Photocrosslinked PEG Bilayers. *Adv. Healthcare Mater.* **2013**, *2*, 1142−1150.
(22) Stuart, M. A. C.; Huck, W. T. S.; Genzer, J.; Muller, M.; Ober, C.; Stamm, M.; Sukhorukov, G. B.; Szleifer, I.; Tsukruk, V. V.; Urban, M.; Winnik, F.; Zauscher, S.; Luzinov, I.; Minko, S. Emerging Applications of Stimuli-Responsive Polymer Materials. *Nat. Mater.* **2010**, *9*, 101−113.
(23) Kumar, K.; Nandan, B.; Formanek, P.; Stamm, M. Fabrication of Carbon Microtubes from Thin Films of Supramolecular Assemblies via Self-Rolling Approach. *J. Mater. Chem.* **2011**, *21*, 10813−10817.
(24) Zakharchenko, S.; Puretskiy, N.; Stoychev, G.; Waurisch, C.; Hickey, S. G.; Eychmuller, A.; Sommer, J. U.; Ionov, L. Stimuli-Responsive Hierarchically Self-Assembled 3d Porous Polymer-Based Structures with Aligned Pores. *J. Mater. Chem. B* **2013**, *1*, 1786−1793.
(25) Stoychev, G.; Turcaud, S.; Dunlop, J. W. C.; Ionov, L. Hierarchical Multi-Step Folding of Polymer Bilayers. *Adv. Funct. Mater.* **2013**, *23*, 2295−2300.
(26) Stoychev, G.; Zakharchenko, S.; Turcaud, S.; Dunlop, J. W. C.; Ionov, L. Shape-Programmed Folding of Stimuli-Responsive Polymer Bilayers. *ACS Nano* **2012**, *6*, 3925−3934.
(27) Kim, J.; Hanna, J. A.; Hayward, R. C.; Santangelo, C. D. Thermally Responsive Rolling of Thin Gel Strips with Discrete Variations in Swelling. *Soft Matter* **2012**, *8*, 2375−2381.
(28) Jamal, M.; Zarafshar, A. M.; Gracias, D. H. Differentially Photo-Crosslinked Polymers Enable Self-Assembling Microfluidics. *Nat. Commun.* **2011**, *2*, 527.
(29) Ghanem, B. S.; Swaidan, R.; Litwiller, E.; Pinnau, I., Ultra-Microporous Triptycene-based Polyimide Membranes for High-Performance Gas Separation. *Adv. Mater.* **2014**, 10.1002/adma.201306229 (accessed 11 Mar **2014**).
(30) Asano, N.; Aoki, M.; Suzuki, S.; Miyatake, K.; Uchida, H.; Watanabe, M. Aliphatic/Aromatic Polyimide Ionomers as a Proton Conductive Membrane for Fuel Cell Applications. *J. Am. Chem. Soc.* **2006**, *128*, 1762−1769.
(31) Agag, T.; Koga, T.; Takeichi, T. Studies on Thermal and Mechanical Properties of Polyimide−Clay Nanocomposites. *Polymer* **2001**, *42*, 3399−3408.
(32) Lan, T.; Kaviratna, P. D.; Pinnavaia, T. J. On the Nature of Polyimide-Clay Hybrid Composites. *Chem. Mater.* **1994**, *6*, 573−575.
(33) Akiyama, M.; Morofuji, Y.; Kamohara, T.; Nishikubo, K.; Ooishi, Y.; Tsubai, M.; Fukuda, O.; Ueno, N. Preparation of Oriented Aluminum Nitride Thin Films on Polyimide Films and Piezoelectric Response with High Thermal Stability and Flexibility. *Adv. Funct. Mater.* **2007**, *17*, 458−462.
(34) Hosono, N.; Yoshikawa, M.; Furukawa, H.; Totani, K.; Yamada, K.; Watanabe, T.; Horie, K. Photoinduced Deformation of Rigid Azobenzene-Containing Polymer Networks. *Macromolecules* **2013**, *46*, 1017−1026.
(35) Liaw, D.-J.; Liaw, B.-Y.; Yu, C.-W. Synthesis and Characterization of New Organosoluble Polyimides Based on Flexible Diamine. *Polymer* **2001**, *42*, 5175−5179.
(36) Stober, W.; Fink, A.; Bohn, E. Controlled Growth of Monodisperse Silica Spheres in Micron Size Range. *J. Colloid Interface Sci.* **1968**, *26*, 62−69.
(37) Wang, C.; Wang, T. M.; Pei, X. Q.; Wang, Q. H. Shell-Core-Corona Aggregates Formed from Poly(Styrene)-Poly(4-Vinylpyridine) Block Copolymer Induced by Added Homopolymer via Interpolymer Hydrogen-Bonding. *Polymer* **2009**, *50*, 5268−5275.
(38) Zhang, Y.; Wang, Q.; Wang, C.; Wang, T. High-Strain Shape Memory Polymer Networks Crosslinked by SiO_2. *J. Mater. Chem.* **2011**, *21*, 9073−9078.
(39) Wang, Q.; Wang, C.; Wang, T. Controllable Low Dielectric Porous Polyimide Films Templated by Silica Microspheres: Microstructure, Formation Mechanism, and Properties. *J. Colloid Interface Sci.* **2013**, *389*, 99−105.
(40) Wang, C.; Wang, Q.; Wang, T. Simple Method for Preparation of Porous Polyimide Film with an Ordered Surface Based on in Situ Self-Assembly of Polyamic Acid and Silica Microspheres. *Langmuir* **2010**, *26*, 18357−18361.
(41) Woodcock, L. V. Entropy Difference Between the Face-Centred Cubic and Hexagonal Close-Packed Crystal Structures. *Nature* **1997**, *385*, 141−143.
(42) Byun, M.; Lin, Z., Self-Assembly of Highly Ordered Structures Enabled by Controlled Evaporation of Confined Microfluids. In *Evaporative Self-Assembly of Ordered Complex Structures*, Lin, Z., Ed.; World Scientific Publishing Co. Pte. Ltd.: Singapore, 2012; pp 295−349.